Directed excitation transfer in vibrating chains by external fields

Oliver Mülken and Maximilian Bauer
Physikalisches Institut, Universität Freiburg, Hermann-Herder Straße 3, DE-79104 Freiburg, Germany
(Received 13 October 2010; revised manuscript received 3 March 2011; published 16 June 2011)

We study the coherent dynamics of excitations on vibrating chains. By applying an external field and matching the field strength with the oscillation frequency of the chain it is possible to obtain an (average) transport of an initial Gaussian wave packet. We distinguish between a uniform oscillation of all nodes of the chain and the chain being in its lowest eigenmode. Both cases can lead to directed transport.

DOI: 10.1103/PhysRevE.83.061123 PACS number(s): 05.60.Gg, 05.60.Cd, 71.35.−y

I. INTRODUCTION

The transport of energy or charge is fundamental for a large variety of physical, chemical, and biological processes. One of the most prominent examples is the energy transfer in the light-harvesting complexes in photosynthesis [1]. There, the energy of the captured solar photons is transported via a molecular backbone to the reaction center where the energy is transformed into chemical energy. Recent experiments have shown that coherent features of the transport process might be crucial for a high efficiency [2,3]. Usually, the system and the dynamics of the excitation (exciton) is modeled by open quantum systems where the system of interest, e.g., the light-harvesting complex, is coupled to an external environment. It has been shown that the environment can also support the coherent dynamics [4–10].

Most of the models assume a time-independent Hamiltonian motivated by the fact that, indeed, the network of chromophores underlying the energy transfer is rather static, even at higher (room) temperatures. However, this need not be the case. One can easily imagine the situation where the underlying molecule is not static but performs some kind of mechanical oscillation. Asadian *et al.* have shown that certain types of motions can enhance the transfer efficiency when compared to the static situation [11]. In a related model, Semião *et al.* studied the modulation of the excitation energies of coupled quantum dots driven by a nanomechanical resonator mode, also enhancing the transport efficiency [12]. Vaziri and Plenio showed that the periodic modulation of ion channels leads to the emergence of resonances in their transport efficiency [13].

Another influence on the dynamics can be external fields. Hartmann *et al.* have shown for the coherent transport of an initial Gaussian wave packet on a discrete (static) chain of nodes that by suitably switching the direction of a constant external field, one can achieve directed transport [14]. There, the switching frequency has been matched with the Bloch oscillation frequency. The effect of Bloch oscillations on the trapping of excitations has been studied by Vlaming *et al.*, finding that the trapping efficiency crucially depends on the strength of the external field (the bias) [15,16].

Clearly, mechanical motions and external fields are not restricted to energy transfer in molecular aggregates. Other examples include cold atoms in optical lattices whose spacings can be periodically modulated [17] or waveguide arrays where the "external field" is achieved by a linear variation of the effective refractive index across the array (see, e.g., [18]).

A question we address in this paper is whether it is possible to engineer the excitation transport in systems performing mechanical oscillations with a constant external field such that also here one obtains directed transport.

II. MODEL

We consider the excitation dynamics on a finite chain of N nodes with time-dependent couplings $J_n(t)$ between two adjacent nodes of the chain. The dynamics will be modeled by continuous-time quantum walks [19], a model motivated by the mathematical similarities between the discrete Schrödinger equation and the classical (diffusive) master equation [20]. In the case of a chain, such a model—sometimes in more complicated forms—is known in various fields of physics [21] and physical chemistry [22] under different names, e.g., "tight-binding model" [23], "hopping model" or "Anderson model" (without disorder) [24], "Bose-Hubbard model" [25,26], or "Frenkel exciton model" [27–29]. A short derivation of the model for time-independent couplings between the nodes can be found, e.g., in Chap. 2.1 of the second part of [29]. It is straightforward to extend this to time-dependent couplings between the nodes such that in second quantization the Hamiltonian can be written as

$$\boldsymbol{H}_0 = \sum_{n=1}^{N} E_n c_n^\dagger c_n + \sum_{n=1}^{N-1} J_n(t)\left(c_n^\dagger c_{n+1} + c_{n+1}^\dagger c_n\right), \qquad (1)$$

where E_n are the site energies which we choose to be equal and constant, i.e., $E_n = E$ [30]; $c_n^\dagger$ and c_n are creation and annihilation operators, creating and annihilating an excitation at node n, respectively. In the node basis $\{|n\rangle,\ n = 1,\ldots,N\}$ we can write $c_n^\dagger = |n\rangle\langle \mathrm{vac}|$ and $c_n = |\mathrm{vac}\rangle\langle n|$, where $|\mathrm{vac}\rangle$ is the "vacuum state" where no excitation is present in the system (note that $\langle \mathrm{vac}|\mathrm{vac}\rangle = 1$). Inserting this into Eq. (1) leads to the following representation of the Hamiltonian:

$$\boldsymbol{H}_0 = \sum_{n=1}^{N} E_n |n\rangle\langle n| + \sum_{n=1}^{N-1} J_n(t)(|n\rangle\langle n+1| + |n+1\rangle\langle n|). \qquad (2)$$

Now, in addition, we apply an external field with strength f, such that the total Hamiltonian for an excitation on a vibrating chain reads

$$\boldsymbol{H}_S = \boldsymbol{H}_0 + f\sum_{n=1}^{N} n|n\rangle\langle n|. \qquad (3)$$

For chains whose nodes (molecules or atoms) interact via dipole-dipole forces, the couplings decay with the third power of the distance between the nodes. Here, on a chain of length L two nodes k and j have positions $(k-1)L/(N-1)$ and $(j-1)L/(N-1)$, respectively, such that their (chemical) distance $r_{kl} = |k-l|L/(N-1)$. Then, two adjacent nodes have $r_{k,k+1} = L/(N-1)$. Now, for dipole-dipole forces, the coupling between next-nearest neighbors is by a factor of $1/8$ smaller than the coupling between nearest neighbors. Therefore, we neglect next-nearest neighbor couplings and consider only nearest neighbor couplings in H_0.

Now, there are two competing effects: On the one hand, excitations in a static chain with an external field perform Bloch oscillations [14,31,32]. On the other hand, the time-dependent couplings can cause an enhanced transport efficiency [11–13]. If the oscillations are periodic, the distances between two adjacent nodes vary in a given interval. Short distances means stronger couplings and thus faster transport from node to node. Longer distances lead to weaker couplings and slower transport. Therefore, matching the Bloch frequency with the frequency of the chain oscillation should lead to an effective transport in one direction along the chain. The reason is that in the first half of the Bloch period T_B the distances between the nodes are smaller, while in the second half of T_B the distances are larger. This leads to different displacements in the two half periods and consequently, to an overall displacement of the inital excitation in one direction.

We choose the same two scenarios as used by Asadian *et al.* [11] for the couplings $J_n(t)$:

(i) Each node of the chain oscillates uniformly with the same frequency ω and with the same amplitude a. The couplings follow now as

$$J_n(t) = J(t) = -V/[1 - 2a\ \sin(\omega t + \phi)]^3. \tag{4}$$

(ii) The chain is in its lowest eigenmode, such that for the qth eigenmode the couplings $J_{n,q}(t)$ between the nth and $(n+1)$st nodes are

$$J_{n,q}(t) = -V/[1 - 2a_{n,q}\ \sin(\omega_q t + \phi)]^3 \tag{5}$$

(see Sec. III C for details).

Clearly, for time-constant $J_n = J$ we recover the known Bloch oscillations with frequency $\omega_B = f/\hbar$ (we set $\hbar = 1$ in the following). Thus, the period of the oscillation $T_B = 2\pi/\omega_B = 2\pi/f$.

The dynamics of an initial excitation is governed by the Liouville–von Neumann equation for the density operator $\boldsymbol{\rho}(t)$. Without any external environment leading to decoherence, the dynamics is fully coherent following

$$\dot{\boldsymbol{\rho}}(t) = -i[\boldsymbol{H}_S, \boldsymbol{\rho}(t)]. \tag{6}$$

Now, if the system is coupled to an environment such that the total Hamiltonian can be split into three parts, $\boldsymbol{H}_{\rm tot} = \boldsymbol{H}_S + \boldsymbol{H}_R + \boldsymbol{H}_{RS}$, where H_R is the Hamiltonian of the environment and H_{RS} is the Hamiltonian of the system-environmental coupling. For small couplings to the environment we will study the dynamics by the Lindblad quantum master equation [33]

$$\dot{\boldsymbol{\rho}}(t) = -i[\boldsymbol{H}_S, \boldsymbol{\rho}(t)] - \lambda \sum_{j=1}^{N} (\boldsymbol{\rho}(t) - \langle j|\boldsymbol{\rho}(t)|j\rangle)|j\rangle\langle j|, \tag{7}$$

where we assumed Lindblad operators of the form $\sqrt{\lambda}|j\rangle\langle j|$. The term proportional to λ mimics the influence of the environment leading to decoherence. In the following we will consider the occupation probabilities $\rho_{kk}(t) \equiv \langle k|\boldsymbol{\rho}(t)|k\rangle$ for a given initial condition $\boldsymbol{\rho}(0)$.

III. RESULTS

In all calculations shown below we used $N = 103$ and an initial Gaussian wave packet centered at $N_c(0) = N_0$ with a standard deviation of $\sigma = 6$. We adjust N_0 such that in the first two periods of the Bloch oscillations the wave packet does not encounter the edges of the chain, such that we can exclude interference effects caused by reflection. We further take $V = 1$.

A. Static chain

We start by considering the static chain, i.e., no oscillations ($a = 0$). Without any external field and no external environment, the dynamics of wave packets on the static chain is very similar to the motion of a quantum particle in a box [34,35]. One can also observe (partial) revivals of initially localized wave packets caused by reflections at the end of the chain, thus obtaining the discrete analog of so-called quantum carpets [36,37].

When applying an external field, the situation changes. Figure 1 shows for $N_0 = 78$ the well-known Bloch oscillations in the occupation probabilities $\rho_{kk}(t)$ with Bloch frequency $\omega_B = f$ for $f = 0.2$ with no external coupling, $\lambda = 0$ (left panel) and with small external coupling, $\lambda = 0.05$ (right panel). One clearly recognizes the oscillation period of $T_B = 2\pi/f = 10\pi$. The coupling to the environment leads to a spreading of the wave packet over more and more nodes as time progresses. Eventually, this will lead to the equilibium distribution.

In a continuous approximation for an infinite line, the position of the center of the wave packet follows for vanishing initial momentum as [14,31,32]

$$\Delta N(t) \equiv N_c(t) - N_0 \simeq -\frac{4V}{f} \sin^2(ft/2). \tag{8}$$

Obviously, there is no transport after integer values of T_B, only after $T_B/2 = \pi/f$ has the wave packet traveled by $|\Delta N(T_B/2)| = 4V/f = 20$ nodes in the direction of the field. We note that by instantly reversing the field after $T_B/2$ the wave packet will continue to move to the left side, such that it is possible to obtain directed transport by switching the field every half-period, see [14] for details.

B. Uniformly oscillating chain

If the chain is not static ($a \neq 0$) but oscillates such that the couplings are given by Eq. (4), it is possible to obtain—on average—a net transport of the wave packet in one direction. However, this will depend on the choice of the field strength f, i.e., on the frequency of the Bloch oscillation, on the phase shift ϕ, and on the amplitude a.

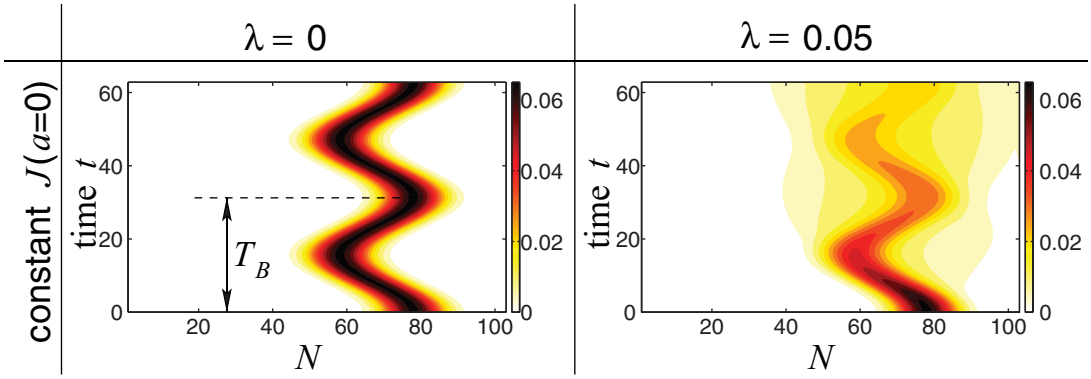

FIG. 1. (Color online) Static chain: Contour plot of the occupation probabilities for $a = 0$ and $f = 0.2$ with $\lambda = 0$ (left panel) and $\lambda = 0.05$ (right panel). Dark (black) regions correspond to large probabilities, while bright (yellow/white) regions correspond to low probabilities.

1. *Analytical approximation*

Before turning to the numerical results, we give an analytical estimate of the displacements $\Delta N_l \equiv [N_c(lT_B) - N_0]$ ($l \in \mathbb{N}$) of the center of the wave packet after integer values of the Bloch period T_B. For the static (infinite) chain, starting from Eq. (8) and differentiating with respect to time, one has

$$\dot{N}(t) = -4V \sin(ft/2)\cos(ft/2) = -2V \sin(ft), \quad (9)$$

which gives the temporal change of the displacement. Thus, the rate of transport from node to node is V. We extend this idea to the oscillating chain and replace the coupling V with the time-dependent coupling $J(t)$. Then, we define the approximate displacements by integrating $\dot{N}(t)$ over integer values of T_B:

$$\Delta N_{l,\text{approx}} \equiv -2V \int_0^{lT_B} dt \, \frac{\sin(ft)}{[1 - 2a \sin(\omega t + \phi)]^3}. \quad (10)$$

For $\omega = f$ this leads to

$$\Delta N_{l,\text{approx}} = -\frac{12l\pi a V \cos\phi}{f(1-4a^2)^{5/2}}. \quad (11)$$

Clearly, the displacement is maximal for $\phi = 0$ and minimal (zero) for $\phi = \pi$. Note that $\Delta N_{l,\text{approx}}$ is only valid for the infinite chain. In the following we will compare $\Delta N_{l,\text{approx}}$ to numerical results obtained from Eq. (7). As we will show, for the uniformly oscillating chain, $\Delta N_{l,\text{approx}}$ agrees very well with the numerical results. Also, for the chain in its lowest eigenmode we will use $\Delta N_{l,\text{approx}}$ as a starting point to define an *ad hoc* fitting function $\Delta N_{l,\text{fit}}$ which also turns out to be in very good agreement with the numerical results.

2. *Numerical results*

Figure 2 shows the occupation probabilities $\rho_{kk}(t)$ for the case $\omega_B = f = \omega = 0.2$ with $a = 0.1$ and for different phase shifts ϕ. Again, the left panels show the results for isolated chains ($\lambda = 0$) and the right panels for small couplings to an external environment ($\lambda = 0.05$). Plots in different rows correspond to different ϕ. Matching f with ω and having no phase shift results —on average—in a directed transport of the initial wave packet in the direction of the field. In the second half of each Bloch period T_B the wave packet moves in the opposite direction. However, this is overcompensated by the motion in the direction of the field in the first half of each period.

The dependence on the phase shift can be expressed by only considering the average displacement ΔN_l. Figure 3 shows the dependence of ΔN_1 and $\Delta N_2/2$ on ϕ for the same parameters as in Fig. 2. We chose the initial condition such that interference effects due to reflections at the boundaries are avoided, i.e., for $\phi = 0$ we take $N_0 = 39$, for $\phi = \pi/2$ we take $N_0 = 52$, and for $\phi = \pi$ we take $N_0 = 78$. Note that this has no influence on the dynamics because the couplings in the chain are translational invariant. We distinguish between ΔN_1 after one and ΔN_2 after two periods because, in general, one cannot expect a linear behavior of ΔN_l in l. However, as it turns out ΔN_l is approximately linear in l for the uniformly oscillating chain.

Changing the phase shift allows one to control the transport: No phase shift ($\phi = 0$) results in values of $\Delta N_1 \approx -21$ after one period. A phase shift of $\phi = \pi/2$ results in a behavior similar to the Bloch oscillations in the static chain, i.e., no transport (see also Fig. 1). Increasing ϕ further leads to a reversed motion, i.e., the wave packet moves "uphill" against the direction of the field. For $\phi = \pi$ the maximal displacement after one period of $\Delta N_1 \approx 21$ is obtained. For the uniformly oscillating chain, the values for $\Delta N_2/2$ coincide with the ones for ΔN_1 leading to the linear behavior $\Delta N_l = l\Delta N_1$. In addition, Fig. 3 shows the analytical estimate of Eq. (10), which agrees with the numerical results.

The magnitude of the displacements ΔN_l also depends on a. Figure 4 shows $\Delta N_l/l$ as a function of a for $N_0 = 52$ and $\phi = 0, \pi/2$, and π. While for $\phi = \pi/2$ there is no displacement after integer values of T_B, the displacements for $\phi = 0$ and for $\phi = \pi$ grow with increasing a. Again, the dashed lines show the approximation $\Delta N_{1,\text{approx}}$, which nicely agrees with the numerical results.

The effect of having directed transport depends on having the field strength in resonance with the chain oscillation frequency. In order to see how crucial the exact matching of f and ω is, we study slightly detuned frequencies ω_B, i.e., a mismatch between ω and f. Figure 5 shows for $\phi = 0$ (leading to maximal ΔN_l for $\omega = f$) and for $\omega = 0.2$ the occupation probabilities $\rho_{kk}(t)$ for different values of f. Note that changing f also changes the Bloch period $T_B = 2\pi/f$,

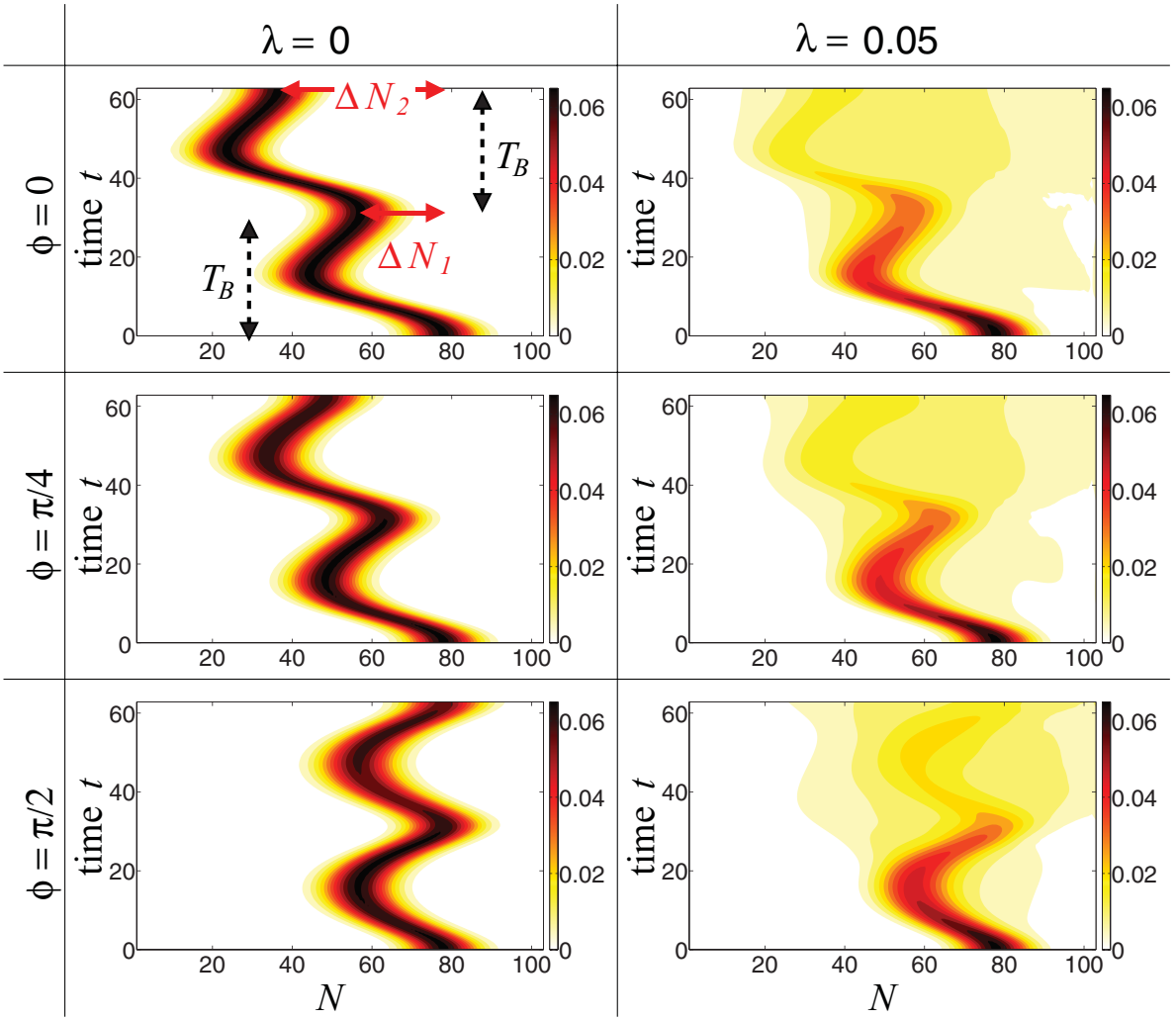

FIG. 2. (Color online) Oscillating chain: Contour plot of the occupation probabilities $\rho_{kk}(t)$ for $a = 0.1$ and $\omega = f = 0.2$ with $\lambda = 0$ (left panels) and $\lambda = 0.05$ (right panels). The three rows correspond to different values of $\phi = 0, \pi/4$, and $\pi/2$, respectively.

thus the time axes are different for different f. A field strength of $f = 0.18$ or $f = 0.22$ reflects a detuning by $\pm 10\%$ of ω. This still results in an average directed transport after two periods of $\Delta N_2 \approx 30$ for $f = 0.18$ and of $\Delta N_2 \approx 36$ for $f = 0.22$. Increasing the detuning further diminishes the transport.

Figure 6 shows the displacements $\Delta N_l/l$ for $\phi = 0$ and different values of f. The maximal displacement is obtained for $\omega \approx f$, as expected. Decreasing or increasing f results in smaller displacements: For $f > \omega$ the decrease in displacement is slower than for $f < \omega$. One also observes that the displacements change direction. For $f < \omega$, $\Delta N_2/2$ changes

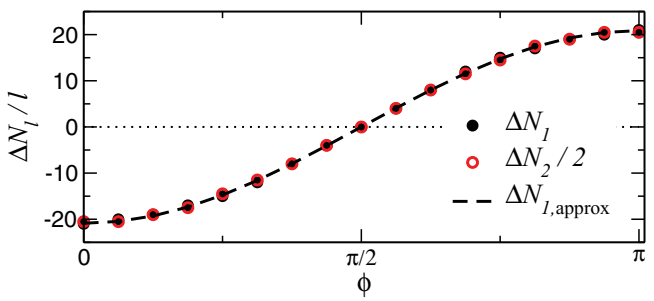

FIG. 3. (Color online) Oscillating chain: Displacements $\Delta N_l/l$ with $l = 1,2$, extracted from the occupation probabilities for $N_0 = 52$, as a function of ϕ for $a = 0.1$, $\omega = f = 0.2$, and $\lambda = 0$. The dashed lines show $\Delta N_{l,\mathrm{approx}}$ given in Eq. (10).

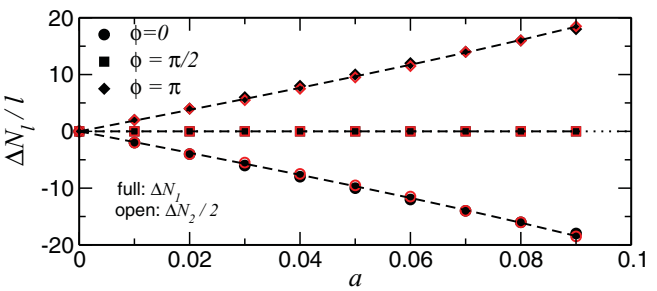

FIG. 4. (Color online) Oscillating chain: Displacements $\Delta N_l/l$ with $l = 1,2$ as a function of a for $\omega = f = 0.2$, $\lambda = 0$, and $\phi = 0, \pi/2, \pi$ with $N_0 = 39$, 52, and 78, respectively. The dashed lines show $\Delta N_{l,\mathrm{approx}}$ given in Eq. (10).

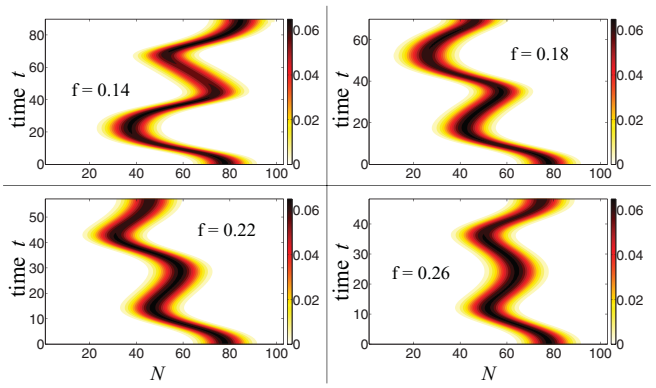

FIG. 5. (Color online) Oscillating chain: Contour plot of the occupation probabilities $\rho_{kk}(t)$ with $\omega = 0.2$, $a = 0.1$, $\phi = 0$, and $\lambda = 0$ for different values of f.

direction at about $f/\omega = 0.8$ and ΔN_1 at about $f/\omega \approx 0.67$. For $f > \omega$, the direction change happens at larger deviations from the resonance condition. Additionally, there are maximal displacements in the opposite direction.

As before, we can obtain an approximation to the numerical results: Considering now $f \neq \omega$ in Eq. (10) and numerically integrating over integer values of the Bloch oscillation yields the dashed curves shown in Fig. 6. Again, the approximation is in very good agreement with the numerical data.

Having now explored a large region of the parameters f/ω, a, and ϕ, we see that the dynamics of an initial Gaussian wave packet can be manipulated by a suitable choice of these parameters: We can make the wave packet move—on average—in one preferred direction by choosing the phase shift ϕ. The magnitude of the displacements in either direction is given by a. Moreover, we do not have to exactly match the Bloch frequency $\omega_B = f$ with the oscillation frequency ω in order to obtain directed transport; there is a fairly large range of roughly $\pm 10\%$ around $f/\omega = 1$ in which large displacements can be obtained.

C. Chain in lowest eigenmode

In contrast to the previous section, we now consider the dynamics on a finite chain in its lowest eigenmode. Although this mode is similar to the uniform oscillation, the finite size of the chain becomes crucial leading to a nonuniform oscillation of the nodes.

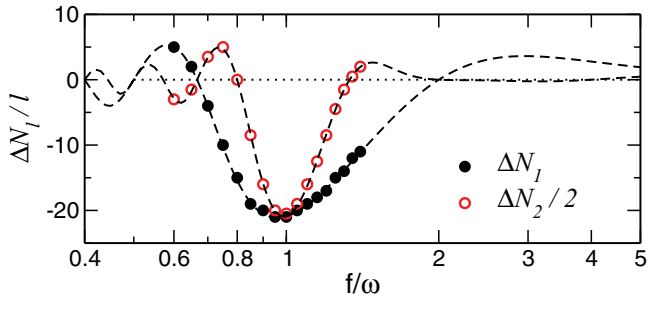

FIG. 6. (Color online) Oscillating chain: Displacements $\Delta N_l/l$ with $l = 1,2$ as a function of f for $a = 0.1$, $\omega = 0.2$, $\phi = 0$, and $\lambda = 0$ (note the semilogarithmic scale). The dashed lines show the approximation obtained by numerical integration (see text for details).

The couplings $J_{n,q}(t)$ in Eq. (5) between the nodes are obtained from a normal mode analysis of a free chain of nodes connected by springs (see [11] for details). Although the motion of the nodes is not uniform [38], there are close similarities to the results presented in the previous section.

In order to obtain comparable results we have to adjust the amplitudes and frequencies according to the couplings $J_{n,q}(t)$ between nodes n and $n+1$ for the qth eigenmode. The couplings in Eq. (5) can be written as

$$J_{n,q}(t) = -V\left[1 - \frac{2a\,\sin[2\omega t\,\sin(q\pi/2N) + \phi]}{\cos(q\pi/2N)} \times \sin(nq\pi/N)\sin(q\pi/2N)\right]^{-3}, \tag{12}$$

such that one has

$$a_{n,q} \equiv \frac{a\,\sin(nq\pi/N)\sin(q\pi/2N)}{\cos(q\pi/2N)} \tag{13}$$

and

$$\omega_q \equiv 2\omega\,\sin(q\pi/2N). \tag{14}$$

Thus, in the following we will use $\omega_q = f$ as the resonance condition for the frequency and the field. For the amplitude $a_{n,q}$ to be comparable to the amplitudes in the previous section, we consider the average absolute value of the amplitudes, i.e.,

$$\bar{a}_q \equiv \frac{1}{N}\sum_{n=1}^{N}|a_{n,q}| = \frac{a}{N}\tan(q\pi/2N)\sum_{n=1}^{N}|\sin(nq\pi/N)| = \frac{aq}{N}\tan(q\pi/2N)\cot(q\pi/2N) = \frac{aq}{N}. \tag{15}$$

Thus, we consider amplitudes $\bar{a}_q$ which—on average—are of the same order as the ones in the previous section. This means that we choose the parameter a in Eq. (13) to be $a = N\bar{a}_q/q$.

Similarly to Fig. 2, Fig. 7 shows the occupation probabilities $\rho_{kk}(t)$ for the case $\omega_B = f = \omega_1$. All plots in Fig. 7 show results for $\bar{a}_1 = 0.04$. We use $\bar{a}_1 = 0.04$ because this clearly avoids interference effects due to reflections at the ends of the chain. Coupling this system to an external environment leads, again, to decoherence and a spreading of the initial wave packet.

Figure 8 shows a comparison of the displacements ΔN_l as a function of the phase shift ϕ for different N_0. Already for the central initial node, $N_0 = 52$ (upper panel), one notices the asymmetry between the behavior of ΔN_1 and $\Delta N_2/2$ for values of $\phi \in [0,\pi/2]$ and values of $\phi \in [\pi/2,\pi]$. For $\phi > \pi/2$ the difference between ΔN_1 and $\Delta N_2/2$ is smaller than for $\phi < \pi/2$ (see, in particular, the points for $\phi = 0$ and $\phi = \pi$). One also notices that $\phi = \pi/2$ yields $\Delta N_l \neq 0$, in contrast to the uniformly oscillating chain. However, the overall behaviors for the two chains are very similar. Therefore, we fit our numerical result for ΔN_1 by a cosine, as suggested by Eq. (10), namely, we use

$$\Delta N_{l,\mathrm{fit}} \equiv \beta_l \frac{\bar{a}_1\,\cos(\phi + \alpha_l)}{\left(1 - 4\bar{a}_1^2\right)^{5/2}}, \tag{16}$$

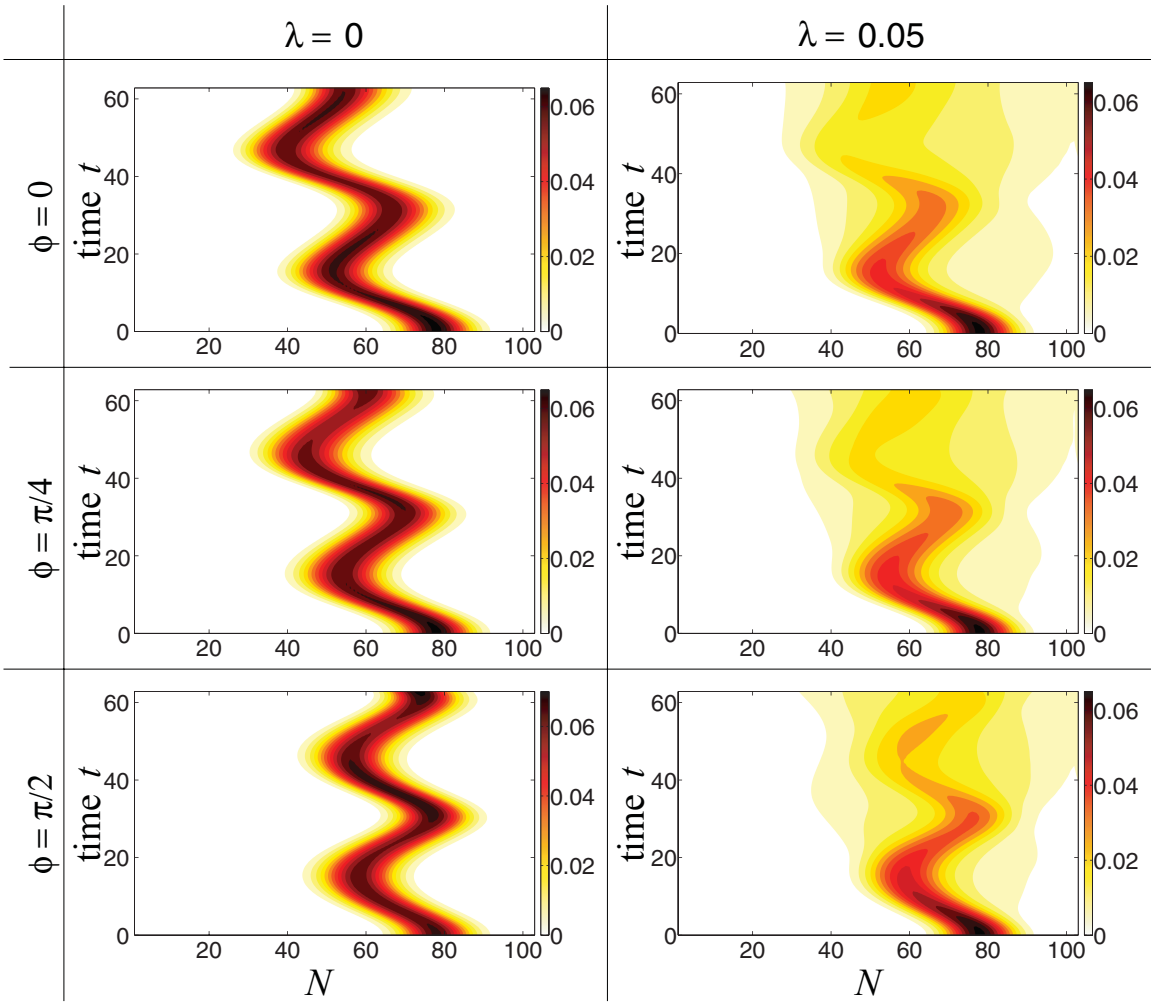

FIG. 7. (Color online) Lowest eigenmode: Contour plot of the occupation probabilities $\rho_{kk}(t)$ for $\bar{a}_1 = 0.04$ and $\omega_1 = f = 0.2$ with $\lambda = 0$ (left panels) and $\lambda = 0.05$ (right panels). The three rows correspond to different values of $\phi = 0, \pi/4$, and $\pi/2$, respectively.

where α_l and β_l are (l-dependent) fit parameters. This already yields very good agreement with the numerical results (see the dashed lines in Fig. 8).

Changing the initial node N_0 influences the behavior of the wave packet. Figure 8 also shows the behavior of ΔN_1 and $\Delta N_2/2$ for $N_0 = 42$ (lower panel, right half) and $N_0 = 78$ (lower panel, left half). While for $N_0 = 52$ one has $|\Delta N_1| \geqslant |\Delta N_2/2|$, one observes for $N = 42$ and for $N_0 = 78$ that $|\Delta N_1| \leqslant |\Delta N_2/2|$. However, for all initial nodes shown in Fig. 8, the maximal displacements (for $\phi = 0$ and $\phi = \pi$) are in the same region about $|\Delta N_l/l| \approx 12$.

The slight asymmetry can be attributed to the nonuniform, i.e., nontranslational invariant, motion of the nodes of the chain and the additional influence of the external field, which breaks the point symmetry with respect to the center.

The $\bar{a}_1$ dependence of the displacements is shown in Fig. 9. Although the absolute values of $\Delta N_l/l$ are different for different N_0, there is a similar behavior for different values of ϕ. Moreover, the behavior is similar to the one for the uniformly oscillating chain (see Fig. 4). Therefore, we fit the $\bar{a}_1$ dependence of ΔN_1 by $\Delta N_{1,\text{fit}}$ given in Eq. (16). Also here are the fits in very good agreement with the numerical results.

Figure 10 shows the displacements ΔN_1 and $\Delta N_2/2$ as a function of f for $\phi = 0$ with $N_0 = 52$. Similar to the oscillating chain, the displacements are maximal for $f \approx \omega_1$. The dashed lines show the approximations obtained for the oscillating chain (see Fig. 6) but rescaled by a factor 1/2. Already this rough approximation yields good agreement to the numerical results. However, the points for $f/\omega = 0.6$ have to be considered with care, because such a detuning leads to interference effects due to reflection at the end node of the chain after one half period. This interference obviously can influence the dynamics of the wave packet.

Now, also for the chain in its lowest eigenmode, we obtain similar results to the ones for the oscillating chain. However, the absolute values of the parameters are different. Nevertheless, the approximations given by Eq. (10) turn out to give qualitatively the correct behavior. Therefore, the same conclusions as for the oscillating chain apply here.

D. Effect of disorder

In order to study the robustness of the directed transport we examine the dynamics of the initial wave packet with diagonal disorder. Biased chains with disorder but without vibrations

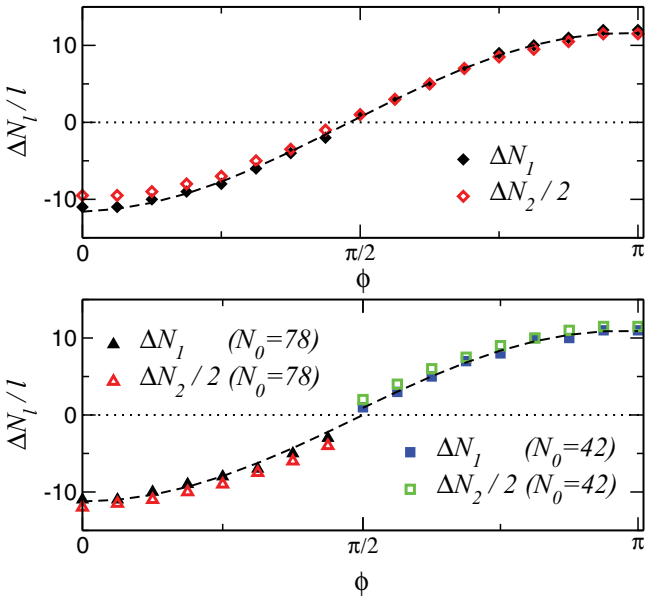

FIG. 8. (Color online) Lowest eigenmode: Displacements $\Delta N_l/l$ with $l = 1,2$ for $N_0 = 52$ (upper panel) and for $N_0 = 42$ and $N_0 = 78$ (lower panel) as a function of ϕ for $\bar{a}_1 = 0.04$, $\omega_1 = f = 0.2$, and $\lambda = 0$. The dashed lines show the fits for $\Delta N_{l,\mathrm{fit}}$ given by Eq. (16).

have been studied before [15]. Here, it was found that for given disorder strength the transport can be tuned by varying the strength of the bias, thus compensating the (Anderson) localization by Bloch oscillations.

Since the uniformly oscillating chain and the chain in its lowest vibrational eigenmode qualitatively behave in a similar way, we exemplify the effect of disorder for the uniformly

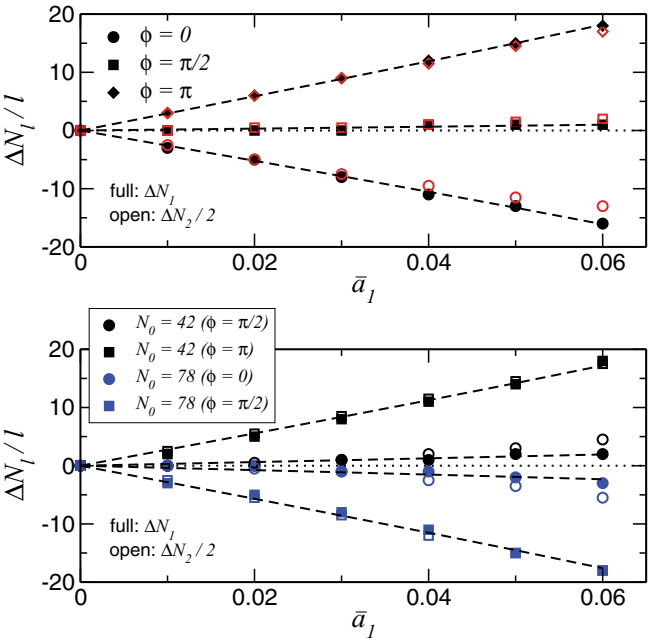

FIG. 9. (Color online) Lowest eigenmode: Displacements $\Delta N_l/l$ with $l = 1,2$ as a function of $\bar{a}_1$ for $\omega_1 = f = 0.2$, and $\lambda = 0$: upper panel for $N_0 = 52$ with $\phi = 0,\pi/2,\pi$ and lower panel for $N_0 = 42$ with $\phi = \pi/2,\pi$ and $N_0 = 78$ with $\phi = 0,\pi/2$. The dashed lines show the fits for $\Delta N_{1,\mathrm{fit}}$ given by Eq. (16).

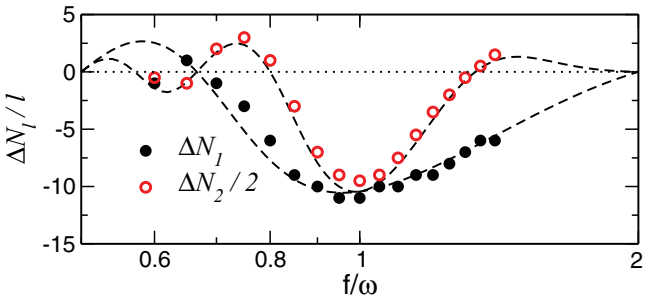

FIG. 10. (Color online) Lowest eigenmode: Displacements $\Delta N_l/l$ with $l = 1,2$ as a function of f for $N_0 = 52$, $\bar{a}_1 = 0.04$, $\omega_1 = 0.2$, $\phi = 0$, and $\lambda = 0$ (note the semilogarithmic scale). The dashed lines show the approximations of Fig. 6 scaled by a factor of 1/2 (see text for details).

oscillating chain with Gaussian disorder of different strengths (standard deviation) σ_d. Here, we consider diagonal (on-site) energetic disorder, i.e., the on-site energies are augmented with uncorrelated random numbers from a Gaussian distribution centered around zero with standard deviation σ_d. We also restrict ourselves to the case where one has—for fixed amplitude a—the most effective directed transport, i.e., we neglect any coupling to an environment ($\lambda = 0$) and we fix $\omega = f = 0.2$ and $\phi = 0$. Figure 11 shows the ensemble-averaged occupation probabilities after two Bloch periods, $\bar{\rho}_{kk}(2T_B)$, for the same system size as above without disorder ($\sigma_d = 0$), and with different strengths (standard deviations) of Gaussian disorder ($\sigma_d = 0.1V,\ldots,1.0V$); the ensemble average runs over 500 realizations.

While with relatively weak disorder ($\sigma_d = 0.1V$) the effect of directed transport is still present, although in the ensemble average the occupation probabilities $\bar{\rho}_{kk}(t)$ do not fully conserve the Gaussian shape (see solid lines), this effect is destroyed for larger disorder. For larger disorder strengths ($\sigma_d = 0.5V$), there is still a remainder of the Bloch oscillation after two Bloch periods, visible as a broad distribution of $\bar{\rho}_{kk}(2T_B)$, which has its maximum on the left-hand side of the initial distribution. Increasing the disorder further ($\sigma_d = 1.0V$)

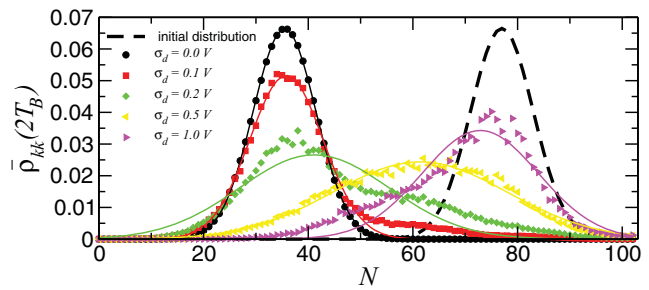

FIG. 11. (Color online) Oscillating chain with Gaussian diagonal disorder: Ensemble averaged occupation probabilities after two Bloch periods T_B, $\bar{\rho}_{kk}(2T_B)$ (symbols), for a chain of length $N = 103$ without disorder ($\sigma_d = 0$), and different strengths (standard deviations) of Gaussian disorder ($\sigma_d = 0.1V,\ldots,1.0V$). All other parameters for the chain are chosen to yield (for $a = 0.1$) the largest deviation after two Bloch periods, i.e., $\omega = f = 0.2$, $\phi = 0$, and $\lambda = 0$. The ensemble average runs over 500 realizations. The solid lines show Gaussian fits to $\bar{\rho}_{kk}(2T_B)$.

results in localization around the initial condition. Therefore, instead of varying the field strength f with fixed disorder strength σ_d as in [15], we find that the directed transport in chains vibrating with frequency ω and with an external field of strength $f = \omega$ crucially depends on the disorder. In particular, weak disorder still allows for directed transport.

Apart from Anderson localization which is due to disorder, it is also known that a time-dependent external field can lead to (dynamic) localization of excitations in static chains [39]. Since in our case a rather sensitive matching of field strength with the chain's vibrational frequency is needed in order to achieve directed transport, we expect that a time-dependent field will hamper, if not prevent, directed transport. A more detailed study of both localization effects will be given elsewhere.

IV. CONCLUSIONS

We have studied the coherent transport of excitations on a finite chain with time-dependent couplings between adjacent nodes of the chain and in the presence of an external field. The field leads to Bloch oscillations, while regular time-dependent couplings can lead to an increased transport efficiency of excitations along the chain. We showed for uniformly oscillating chains and for a chain in its lowest eigenmode that matching the Bloch oscillation frequency with the frequency of the chain leads to an (average) directed displacement of an initial Gaussian wave packet, even for weak disorder. Applying a phase difference allows one to manipulate the direction of the transport, while changing the amplitude of the regular oscillation allows one to manipulate the strength of the displacements. We corroborate our findings by an analytic (continuous) approximation for the average displacement of an initial Gaussian wave packet in an infinite chain after integer values of the Bloch period. For the uniformly oscillating chain, this ansatz yields a functional form for the displacements, which agrees very well with the numerical data. Using the same functional form also allows one to define a fitting function for the chain in its lowest eigenmode, also leading to very good agreement with the numerical results. In both cases, interference effects due to reflections at the ends of the chains have been neglected.

ACKNOWLEDGMENTS

Support from the Deutsche Forschungsgemeinschaft (DFG) is gratefully acknowledged. We thank Alexander Blumen for continuous support and fruitful discussions.

[1] G. R. Fleming and G. D. Scholes, Nature (London) **431**, 256 (2004).
[2] G. S. Engel, T. R. Calhoun, R. L. Read, T.-K. Ahn, T. Mancal, Y.-C. Cheng, R. E. Blankenship, and G. R. Fleming, Nature (London) **446**, 782 (2007).
[3] E. Collini, C. Y. Wong, K. E. Wilk, P. M. G. Curmi, P. Brumer, and G. D. Scholes, Nature (London) **463**, 644 (2010).
[4] Y. C. Cheng and R. J. Silbey, Phys. Rev. Lett. **96**, 028103 (2006).
[5] M. Mohseni, P. Rebentrost, S. Lloyd, and A. Aspuru-Guzik, J. Chem. Phys. **129**, 174106 (2008).
[6] M. B. Plenio and S. F. Huelga, New J. Phys. **10**, 113019 (2008).
[7] F. Caruso, A. W. Chin, A. Datta, S. F. Huelga, and M. B. Plenio, J. Chem. Phys. **131**, 105106 (2009).
[8] A. Olaya-Castro, C. F. Lee, F. F. Olsen, and N. F. Johnson, Phys. Rev. B **78**, 085115 (2008).
[9] M. Thorwart, J. Eckel, J. Reina, P. Nalbach, and S. Weiss, Chem. Phys. Lett. **478**, 234 (2009).
[10] O. Mülken and T. Schmid, Phys. Rev. E **82**, 042104 (2010).
[11] A. Asadian, M. Tiersch, G. G. Guerreschi, J. Cai, S. Popescu, and H. J. Briegel, New J. Phys. **12**, 075019 (2010).
[12] F. L. Semião, K. Furuya, and G. J. Milburn, New J. Phys. **12**, 083033 (2010).
[13] A. Vaziri and M. B. Plenio, New J. Phys. **12**, 085001 (2010).
[14] T. Hartmann, F. Keck, H. J. Korsch, and S. Mossmann, New J. Phys. **6**, 2 (2004).
[15] S. M. Vlaming, V. A. Malyshev, and J. Knoester, J. Chem. Phys. **127**, 154719 (2007).
[16] S. M. Vlaming, V. A. Malyshev, and J. Knoester, J. Lumin. **128**, 956 (2008).
[17] S. Al-Assam, R. A. Williams, and C. J. Foot, Phys. Rev. A **82**, 021604 (2010).
[18] D. N. Christodoulides, F. Lederer, and Y. Silberberg, Nature (London) **424**, 817 (2003).
[19] O. Mülken and A. Blumen, Phys. Rep. **502**, 37 (2011).
[20] E. Farhi and S. Gutmann, Phys. Rev. A **58**, 915 (1998).
[21] R. P. Feynman, R. B. Leighton, and M. Sands, in *The Feynman Lectures on Physics*, Quantum Mechanics Vol. III (Addison-Wesley, Reading, MA, 1964).
[22] D. A. McQuarrie, *Quantum Chemistry* (Oxford University Press, Oxford, 1983).
[23] J. Sakurai, *Modern Quantum Mechanics*, 2nd ed. (Addison-Wesley, Redwood City, CA, 1994).
[24] P. W. Anderson, Rev. Mod. Phys. **50**, 191 (1978).
[25] F. H. L. Essler, H. Frahm, F. Göhmann, A. Klümper, and V. E. Korepin, *The One-Dimensional Hubbard Model* (Cambridge University Press, Cambridge, England, 2005).
[26] A. Altland and B. Simons, *Condensed Matter Field Theory* (Cambridge University Press, Cambridge, England, 2006).
[27] S. Mukamel, *Principles of Nonlinear Optical Spectroskopy* (Oxford University Press, New York, 1995).
[28] V. May and O. Kühn, *Charge and Energy Transfer Dynamics in Molecular Systems* (Wiley-VCH, Weinheim, 2004).
[29] V. M. Kenkre and P. Reineker, *Exciton Dynamics in Molecular Crystals and Aggregates* (Springer, Berlin, 1982).
[30] Here we use the continuous-time quantum walk convention that the diagonal element for a given node n is equal to the sum of the connections emanating from n, i.e., we have $E_n = 2$ for all nodes $n = 2, \ldots, N-1$ of the chain except the two end nodes where we have $E_n = 1$ for $n = 1, N$. Assuming $E_n = E$ for all nodes does not considerably change the dynamics for the chain lengths considered here.
[31] M. Holthaus and D. W. Hone, Philos. Mag. B **74**, 105 (1996).

[32] H. Fukuyama, R. A. Bari, and H. C. Fogedby, Phys. Rev. B **8**, 5579 (1973).
[33] H.-P. Breuer and F. Petruccione, *The Theory of Open Quantum Systems* (Oxford University Press, Oxford, England, 2006).
[34] O. Mülken and A. Blumen, Phys. Rev. E **71**, 036128 (2005).
[35] O. Mülken and A. Blumen, Phys. Rev. A **73**, 012105 (2006).
[36] W. Kinzel, Phys. Bl. **51**, 1190 (1995).
[37] F. Grossmann, J.-M. Rost, and W. P. Schleich, J. Phys. A **30**, L277 (1997).
[38] H. B. Rosenstock, J. Chem. Phys. **23**, 2415 (1955).
[39] D. H. Dunlap and V. M. KenkrePhys. Rev. B **34**, 3625 (1986).